

Electrophysiology of Flounder Intestinal Mucosa

II. Relation of the Electrical Potential Profile to Coupled NaCl Absorption

DAN R. HALM, EDWARD J. KRASNY, JR., and
RAYMOND A. FRIZZELL

From the Department of Physiology and Biophysics, University of Alabama at Birmingham, Birmingham, Alabama 35294; and Mount Desert Island Biological Laboratory, Salsbury Cove, Maine 04672

ABSTRACT We characterized the hyperpolarization of the electrical potential profile of flounder intestinal cells that accompanies inhibition of NaCl co-transport. Several observations indicate that hyperpolarization of ψ_a and ψ_b ($\Delta\psi_{a,b}$) results from inhibition of NaCl entry across the apical membrane: (a) the response was elicited by replacement of mucosal solution Cl or Na by nontransported ions, and (b) mucosal bumetanide or serosal cGMP, inhibitors of NaCl influx, elicited $\Delta\psi_{a,b}$ and decreased the transepithelial potential (ψ_t) in parallel. Regardless of initial values, ψ_a and ψ_b approached the equilibrium potential for K (E^K) so that in the steady state following inhibition of NaCl entry, $\psi_a \cong \psi_b \cong E^{Cl} \cong E^K$. Bumetanide decreased cell Cl activity (a_c^{Cl}) toward equilibrium levels. Bumetanide and cGMP decreased the fractional apical membrane resistance (f_a^R), increased the slope of the relation of ψ_a to $[K]_m$, and decreased cellular conductance (G_c) by ~85%, which indicates a marked increase in basolateral membrane conductance (G_b). Since the basolateral membrane normally shows a high conductance to Cl, a direct relation between apical salt entry and G_b^{Cl} is suggested by these findings. As judged by the response to bumetanide or ion replacement in the presence of mucosal Ba, inhibition of Na/K/Cl co-transport alone is not sufficient to elicit $\Delta\psi_{a,b}$. This suggests the presence of a parallel NaCl co-transport mechanism that may be activated when Na/K/Cl co-transport is compromised. The $\Delta\psi_{a,b}$ response to reduced apical NaCl entry would assist in maintaining the driving force for Na-coupled amino acid uptake across the apical membrane as luminal [NaCl] falls during absorption.

INTRODUCTION

In the companion paper (10), we summarized the conductance properties of flounder intestinal cells, determined largely from the influence of the bathing solution ion composition on the cellular electrical potential profile. Our findings

Address reprint requests to Dr. D. R. Halm, Dept. of Physiology and Biophysics, University of Alabama at Birmingham, University Station, Birmingham, AL 35294.

revealed a Ba-sensitive K conductance at the apical membrane that underlies the capacity of this tissue for active K secretion (6). The basolateral membrane displays Cl conductance behavior and these pathways contribute to net Cl movement across this barrier during NaCl absorption.

In attempting to evaluate the apical membrane conductance properties, we found that replacement of mucosal solution Na or Cl by impermeant substitutes elicited hyperpolarization of the apical and basolateral membrane potentials, ψ_a and ψ_b . Since NaCl absorption across flounder intestine involves a coupled entry process at the apical membrane, these findings were consistent with an effect of NaCl co-transport on the electrical potential profile. Similar results have been reported for other NaCl-absorbing epithelia, including the diluting segments of *Amphiuma* (18) and *Ambystoma* (22) kidneys, the cortical thick ascending limb of rabbit nephron (9), *Necturus* gallbladder (8), and the intestine of a European teleost, the plaice (13).

Several mechanistic explanations can be offered for the hyperpolarization of the electrical potential profile that results from inhibition of co-transport activity: (a) decreased cell Cl activity (9), which enhances the electromotive force (emf) influencing the potential difference (ψ_b) across the Cl-conductive basolateral membrane, (b) inhibition of an electrogenic NaCl entry process (22) that mediates net positive current flow from mucosal solution to cell, and (c) a reduction in cell volume (27), which could elevate cell K activity and thereby increase the emf across the K-selective apical membrane. A primary alteration of apical or basolateral membrane emf, which all of these interpretations feature, elicits hyperpolarization of the electrical potential differences across both limiting membranes because of current flow via the highly conductive paracellular pathway (10).

This report describes the results of ion-replacement and inhibitor studies illustrating the relation between apical co-transport activity and the electrical potential profile across flounder intestinal cells. The processes leading to hyperpolarization of ψ_a and ψ_b during co-transport inhibition, the involvement of conductance changes in this response, and the physiological implications for intestinal nutrient absorption are discussed.

METHODS

The materials and techniques used to monitor the electrical potential profile, relative membrane resistances, and intracellular Cl activities of flounder intestinal cells are detailed in the companion paper (10). In addition to the standard Ringer's, a solution was designed to approximate the electrolyte composition of the intestinal contents during absorption (12, 14, 19, 24) and contained (mM): 30 Na, 27 *N*-methyl-D-glucamine (NMG), 81 Cl, 5 K, 10 Ca, 100 Mg, 100 SO₄, 5 EPPS, and 5 mannitol; in some experiments, [K] was increased to 30 mM at the expense of NMG. This artificial intestinal fluid (AIF) was used only on the mucosal side and had an osmolarity of 350 mosmol/liter, which was identical to the standard Ringer's solution.

RESULTS

Inhibition of NaCl Absorption

Several conditions that inhibit NaCl absorption also lead to hyperpolarization of ψ_a , as shown in Fig. 1. The degree of hyperpolarization ($\Delta\psi_a$) observed on

addition of bumetanide to, or removal of Cl, Na, or K from, the mucosal solution is similar. Since the primary mechanism that facilitates salt absorption across the apical membrane is a bumetanide-sensitive Na/K/Cl co-transport process (16), these findings imply that inhibition of salt entry elicits hyperpolarization of ψ_a .

This notion is also supported by the results illustrated in Fig. 2, where $\Delta\psi_a$ was examined over a range of mucosal bumetanide concentrations. As the bumetanide concentration increased, ψ_i approached zero and ψ_a hyperpolarized. The half-maximal concentration of bumetanide required for hyperpolarization of ψ_a or inhibition of ψ_i was $\sim 3 \mu\text{M}$. These parallel effects of bumetanide support the notion that $\Delta\psi_a$ results from inhibition of NaCl entry.

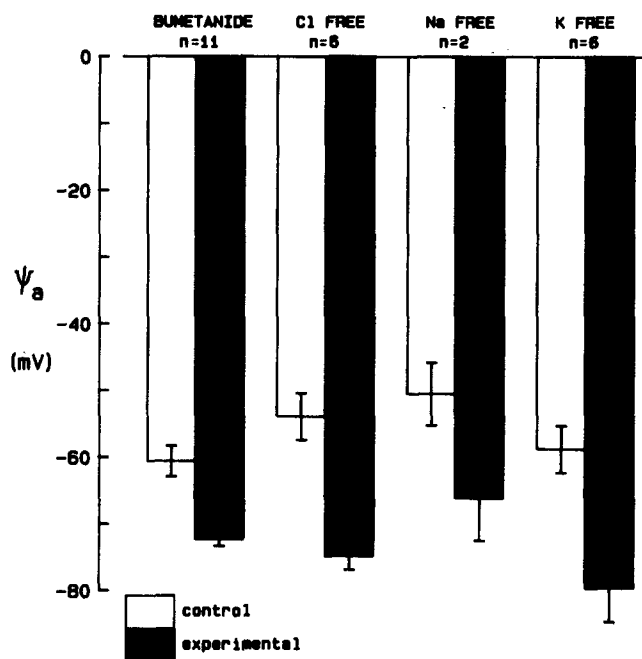


FIGURE 1. Effects of mucosal bumetanide (10^{-4} M) and ion replacement on ψ_a . The mucosal solution alone was rendered Cl- or K-free by replacement with gluconate or Na, respectively. In the Na-free studies, mucosal and serosal solution Na was replaced by NMG. Means \pm SEM are provided, except for the Na-free values, where the range is given.

Hyperpolarization in the Presence of Mucosal Ba

While the effects of K removal (Fig. 1) conform to the notion that inhibition of Na/K/Cl co-transport hyperpolarizes ψ_a in flounder intestine, the increase in E_a^K that occurs with K replacement would hyperpolarize ψ_a in the absence of transport inhibition (cf. Fig. 6, preceding paper). Addition of Ba to the mucosal solution depolarizes ψ_a and increases f_a^R by inhibiting apical K conductance, G_a^K . As f_a^R increases, ψ_a shifts toward the equilibrium potential for Cl across the basolateral membrane, $E_b^{Cl} \cong 40$ mV (10). The results illustrated in Fig. 2 were

obtained in the presence of mucosal Ba, as evidenced by the control ψ_a value (approximately -40 mV).

Since transport inhibition elicits $\Delta\psi_a$ in the presence of mucosal Ba, the effects of ion replacement were re-examined in an attempt to resolve the hyperpolarization elicited by K replacement. Fig. 3 provides results from four groups of tissues in which mucosal Ba depolarized ψ_a to about -40 mV. Subsequent exposure to bumetanide or solutions with reduced [Cl] or [Na] hyperpolarized ψ_a to control (pre-Ba) levels, but K replacement did not.

Fig. 4 shows a record from one of these experiments in which $\Delta\psi_a$ was 4 mV in response to K removal. The results are consistent with a fairly effective

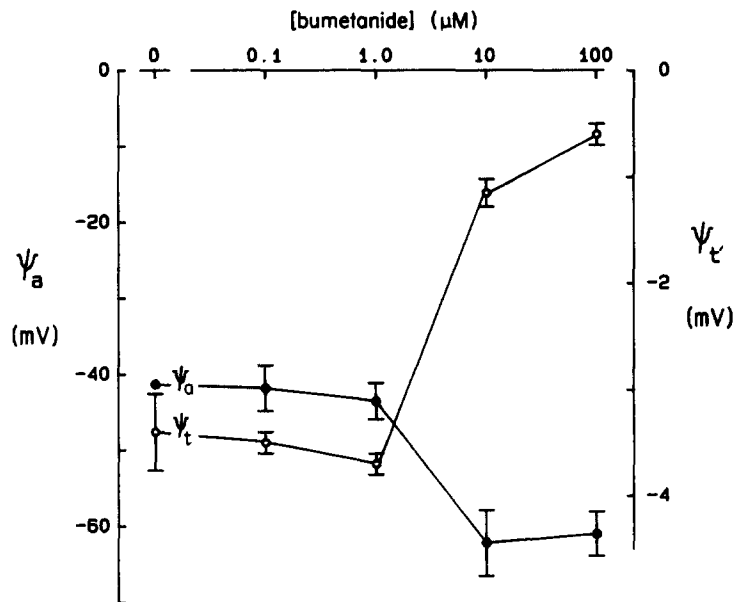


FIGURE 2. Relation of ψ_a and ψ_t to mucosal bumetanide concentration. The means \pm SEM of three to five impalements at each concentration were recorded in a representative experiment. The mucosal solution contained 2 mM Ba throughout.

blockade of apical K conductance by mucosal Ba in the range 0–5 mM $[K]_m$ (see also Fig. 6 of the preceding paper) and suggest that the $\Delta\psi_a$ evoked by K replacement in the absence of Ba (Fig. 1) is due to the increased E_a^K across apical K channels rather than to inhibition of NaCl absorption. The addition of bumetanide to Ba-containing, K-free mucosal solutions hyperpolarized ψ_a by 14 ± 1 mV ($n = 4$). Thus, in the presence of Ba, K-free media do not evoke the (~ 20 mV) $\Delta\psi_a$ observed with other transport inhibitors (Fig. 3), but K replacement does not interfere with the effect of bumetanide on ψ_a . Fig. 4 also shows that ψ_t decreased by only 40% during mucosal K replacement, which suggests that a fraction of NaCl absorption continues when the mucosal solution is K-free.

Fig. 5 shows the response to reduced $[Cl]_m$ in the presence of mucosal Ba. The

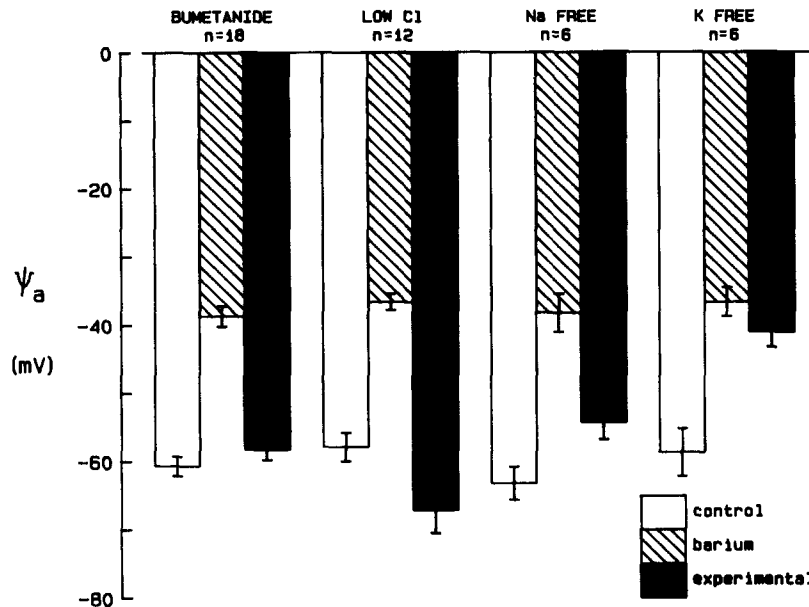


FIGURE 3. Effects of mucosal bumetanide (10^{-4} M) and ion replacement on ψ_a in the presence of mucosal Ba. See the legend of Fig. 1 for details of solution composition. In the Cl substitution studies, $[Cl]_m$ was 4 mM. The data labeled "barium" and "experimental" were obtained with 2 mM Ba in the mucosal solution.

time course of ψ_a is biphasic. The initial depolarization is the response expected for replacement of a permeant anion in the mucosal solution. It probably arises from the bi-ionic (Cl:gluconate) potential generated across the paracellular pathway since its time course parallels that of ψ_t and its magnitude (4 mV) is related

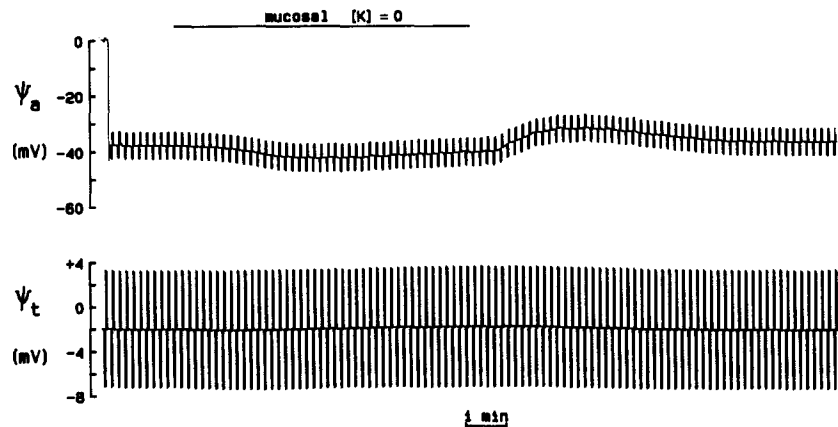


FIGURE 4. Experimental records of ψ_a and ψ_t obtained during replacement of K (by Na). The cell impalement is shown at the beginning of the ψ_a record. Deflections in ψ_a and ψ_t result from passage of bipolar, constant-current pulses across the epithelium to monitor f_a^R . The mucosal solution contained 2 mM Ba throughout.

to ψ_t as predicted by the measured f_a^R (see Eq. 5, preceding paper). The subsequent hyperpolarization of ψ_a is slower than that anticipated for simple conductance behavior (for example, the response to elevated mucosal K; see Fig. 5 of the preceding paper) and is associated with a decrease in ψ_t toward zero, which follows a similar time course. The hyperpolarization of ψ_a (~ 40 mV) is paralleled by a smaller change in ψ_t (~ 4 mV), which implies a primary alteration in the cellular pathway; both $\Delta\psi_a$ and $\Delta\psi_t$ reflect the time course of transport inhibition (see also Fig. 1 and reference 16).

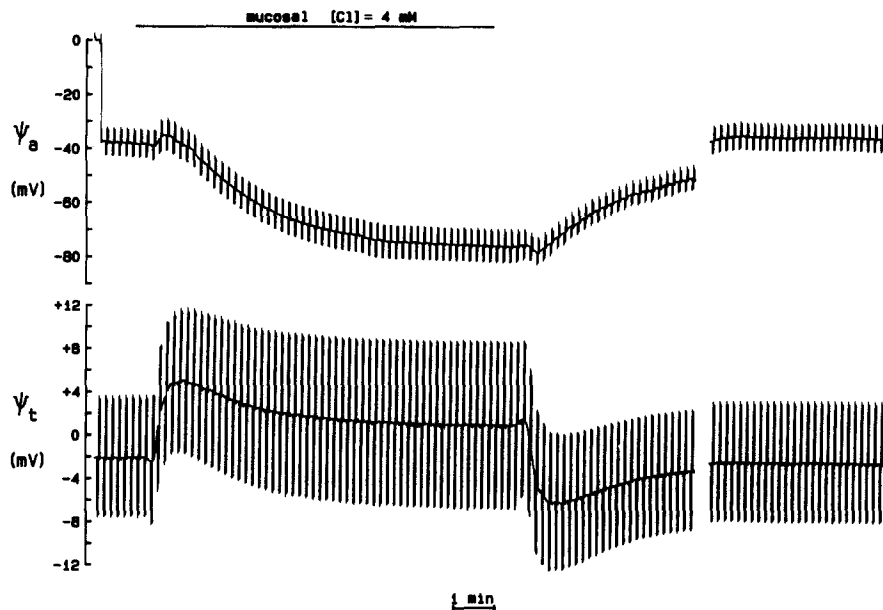


FIGURE 5. Experimental records of ψ_a and ψ_t obtained during reduction of $[Cl^-]_m$ from its normal value of 170 to 4 mM and return. The break in the record is 8 min, during which the impalement was maintained. The mucosal solution contained 2 mM Ba throughout. See the legend of Fig. 4 for other details.

Dependence of ψ_a on Mucosal Solution Ion Concentrations

The kinetics of the relation between co-transport activity and $\Delta\psi_a$ were determined at a variety of mucosal solution Cl, Na, and K concentrations. These experiments were carried out in the presence of 2 mM mucosal Ba to accentuate the $\Delta\psi_a$. The record from an experiment in which $[Cl^-]_m$ was progressively lowered to a final value of 4 mM is illustrated in Fig. 6. As $[Cl^-]_m$ was replaced by gluconate, ψ_a hyperpolarized in a concentration-dependent manner and ψ_t remained relatively constant, which reflects a parallel inhibition of transepithelial salt transport as $[Cl^-]_m$ is lowered. Results similar to these were obtained when $[Cl^-]_m$ was systematically increased or randomly varied.

The high cation selectivity of the paracellular pathway produces large diffusion potentials during unilateral Na replacement (~ 30 mV when one side is rendered Na-free). Therefore, the concentration dependence of $\Delta\psi_a$ was studied using

parallel changes in $[Na]_m$ and $[Na]_s$. The results were qualitatively similar to those obtained from Cl replacement, but the responses were smaller on the average (Fig. 3).

Fig. 7 summarizes the concentration dependence of ψ_a in Ba-treated tissues. The fact that $\Delta\psi_a$ was smaller with Na (compared with Cl) replacement could be due to the use of bilateral Na substitutions, but a more significant factor may be the difference in K_m values of the apical co-transport process, which shows a K_m of 3 mM for Na, whereas that for Cl is ~ 10 times higher (17). Thus, during Na substitution, co-transport activity may be maintained partially by a low Na

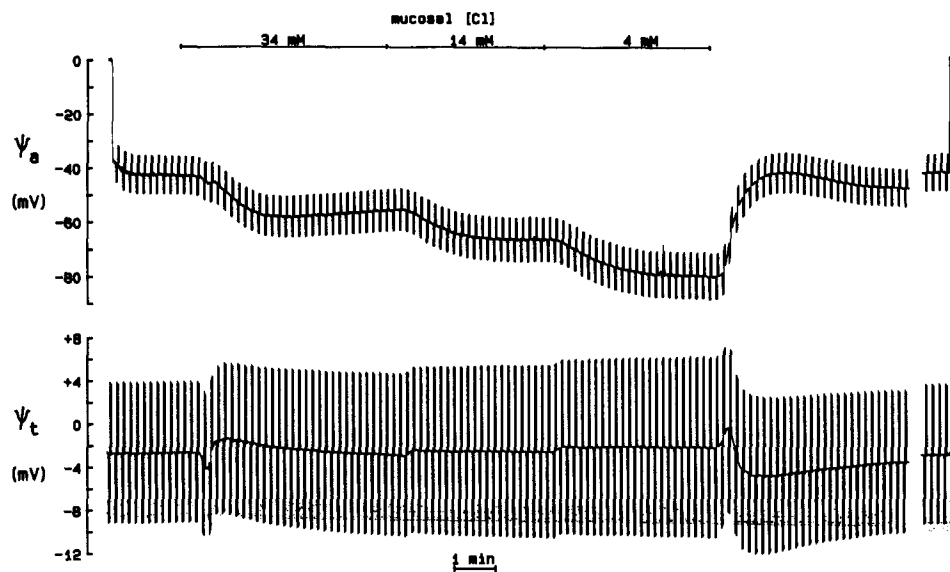


FIGURE 6. Experimental records of ψ_a and ψ_t obtained during progressive reduction in $[Cl]_m$ to the values shown. The break in the record is 9 min, during which the impalement was maintained. The mucosal solution contained 2 mM Ba throughout. For other details, see the legend of Fig. 4.

concentration adjacent to the apical membrane. A more effective Cl replacement is achieved because of inherent differences in co-transport affinities.¹ In the presence of Ba, variations in $[K]_m$ did not affect ψ_a , in agreement with the results of Figs. 3 and 4.

Attempts to Mimic the In Vivo Luminal Composition

During absorption, the ionic composition of the fluid in the intestinal lumen is altered in vivo (12, 14, 19, 24). Isosmotic absorption of NaCl and water reduces luminal $[NaCl]$ while concentrating the nontransported ions Mg, Ca, and SO_4 , ingested with sea water. We prepared an artificial intestinal fluid (AIF; see

¹ The abscissa of Fig. 7 can be converted to relative NaCl entry rate (J/J_{max}) using these K_m values and the $[Na]_m$ and $[Cl]_m$ employed in these experiments. The resulting relation between ψ_a and entry rate is independent of the ion-replacement conditions (Na or Cl).

Methods) to mimic the salt concentrations found at mid-intestine during absorption.

As shown in Table I, when AIF replaced the standard mucosal solution (which continued to bathe the serosal surface), ψ_t increased, G_t decreased, and ψ_a hyperpolarized. The decrease in G_t and increase in ψ_t can be expected from the unilateral reduction in $[\text{Na}]_m$ to 30 mM since the paracellular pathway exhibits a high conductance to Na (7). The hyperpolarization of ψ_a with AIF probably

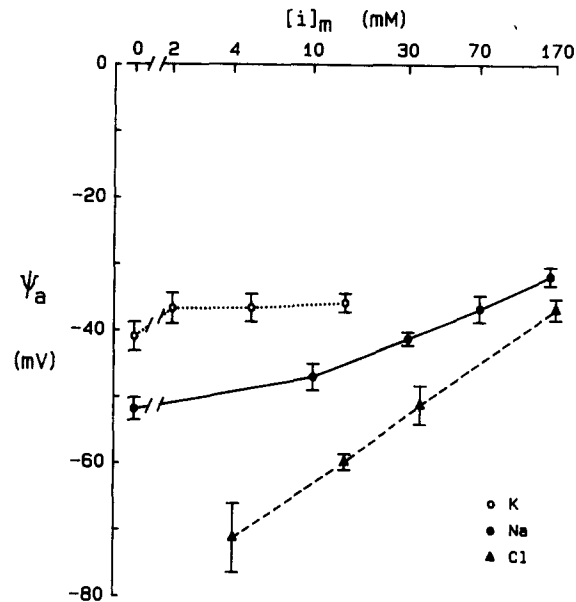


FIGURE 7. Relation of ψ_a to $[\text{Na}]_m$, $[\text{Cl}]_m$, and $[\text{K}]_m$ in the presence of mucosal Ba (2 mM). Means \pm SEM of values from five tissues for $\Delta[\text{Na}]_m$, seven tissues for $\Delta[\text{Cl}]_m$, and six tissues for $\Delta[\text{K}]_m$ are provided. Data were obtained from records like that illustrated in Fig. 6.

results from co-transport inhibition since $[\text{Cl}]_m$ and $[\text{Na}]_m$ are reduced to 81 and 30 mM, respectively. Indeed, the 18-mV hyperpolarization of ψ_a is approximately that expected if the effects of reduced $[\text{Cl}]_m$ and $[\text{Na}]_m$ are additive (Fig. 7).² Inhibition of co-transport activity by Mg, as reported by Ellory (4) in red cells, may also contribute to $\Delta\psi_a$.

In the presence of AIF, the apical membrane retained its K selectivity. The slope of the relation between ψ_a and $[\text{K}]_m$ was 42 mV/decade at $[\text{K}]_m$ between 5 and 30 mM (data not shown). Lowering $[\text{K}]_m$ to 1 mM, a value close to that

² As ψ_t becomes more negative because of a paracellular emf (E_p), ψ_a will hyperpolarize and ψ_b will depolarize in accordance with the relative apical and basolateral membrane resistances (Eqs. 5 and 6 of the preceding paper). If $\Delta\psi_t$ were ascribed entirely to the paracellular pathway, ψ_a would hyperpolarize by 5 mV, while ψ_b would depolarize by 13 mV. Thus, a primary alteration in E_p cannot account for a $\Delta\psi_a$ of 18 mV but may have offset the $\Delta\psi_b$ normally associated with transport inhibition.

TABLE I
Effect of AIF on the Electrical Properties of Flounder Intestine

	ψ_t mV	ψ_a mV	ψ_b mV	f_a^R	G_t mS/cm ²
Control	-3.5±0.5	-64±8	-60±9	0.20±0.01	28.1±5.3
AIF	-21.0±2.1*	-82±3*	-61±1	0.27±0.12	15.1±2.0*

Means ± SEM of values obtained in three tissues exposed sequentially to the standard Ringer's solution and AIF (mucosal surface only).

* $P < 0.05$ compared to control.

found in vivo (12, 19), hyperpolarized ψ_a to -106 ± 4 mV ($n = 3$). The Ba sensitivity of ψ_a could not be assessed, however, since Ba precipitated from AIF, probably as the insoluble salt BaSO₄. Nevertheless, the electrophysiologic consequences of a luminal fluid whose composition resembles that found during absorption are consistent with the results of our studies where [Na]_m and [Cl]_m were varied independently. The implications of these findings for intestinal nutrient absorption will be discussed below.

Effects of Cyclic Nucleotides

From the results of previous studies (15, 21), cAMP and cGMP are known to modify electrolyte transport across flounder intestine in different ways. The primary action of cAMP is to abolish the cation selectivity of the paracellular pathway by specifically increasing its conductance to anions (15). In contrast, the principal site of action of cGMP is inhibition of Na/K/Cl co-transport at the apical membrane (21). Whereas cGMP has no effect on paracellular selectivity, cAMP partially reduces NaCl uptake, perhaps by nonspecifically increasing cellular cGMP.

The actions of the 8-bromo derivatives of cGMP and cAMP on the electrical properties of flounder intestine in the presence and absence of mucosal Ba are summarized in Table II. The effects of cGMP mimic those of bumetanide, reducing ψ_t and hyperpolarizing ψ_a in both the presence and absence of mucosal Ba (compare these results with those of Figs. 1–3 for bumetanide). These findings provide another illustration of the interaction between co-transport activity and

TABLE II
Effects of cGMP and cAMP on the Electrical Properties of Flounder Intestine in the Presence and Absence of Mucosal Ba

	ψ_t mV	ψ_a mV	f_a		ψ_t mV	ψ_a mV	f_a
Control	-2.0±0.3	-57±3	0.35±0.12	Control	-1.9±0.3	-63±3	0.18±0.04
With cGMP	-0.2±0.3*	-71±2*	0.20±0.04	With cAMP	-1.5±0.3*	-64±3	0.22±0.07
Mucosal Ba	-1.3±0.2	-42±3	0.64±0.12	Mucosal Ba	-2.1±0.3	-38±2	0.50±0.13
With cGMP	+0.2±0.2*	-68±1*	0.53±0.15*	With cAMP	-1.6±0.2*	-38±4	0.51±0.14

Means ± SEM of values obtained in five control and three Ba-treated tissues. The 8-bromo derivatives of the cyclic nucleotides were added to the serosal solution alone; 0.05 mM cGMP; 0.5 mM cAMP. The mucosal solution Ba concentration was 2 mM.

* $P < 0.05$ compared to control or Ba as appropriate.

ψ_a . In contrast, cAMP was less effective in reducing ψ_t and had no influence on ψ_a in either the presence or absence of mucosal Ba. The effect of cAMP on flounder intestine differs from that on *Necturus* gallbladder, where it increases apical membrane Cl conductance (2, 20), resembling the action of this agent on Cl-secreting epithelia (5).

Involvement of emf and Conductance Changes in the Response to Transport Inhibition

Fig. 8 illustrates the relation between control ψ_a values and the hyperpolarization ($\Delta\psi_a$) induced by mucosal bumetanide. When ψ_a was -60 to -70 mV, $\Delta\psi_a$ was small. Conversely, tissues with spontaneously low ψ_a values hyperpolarized by

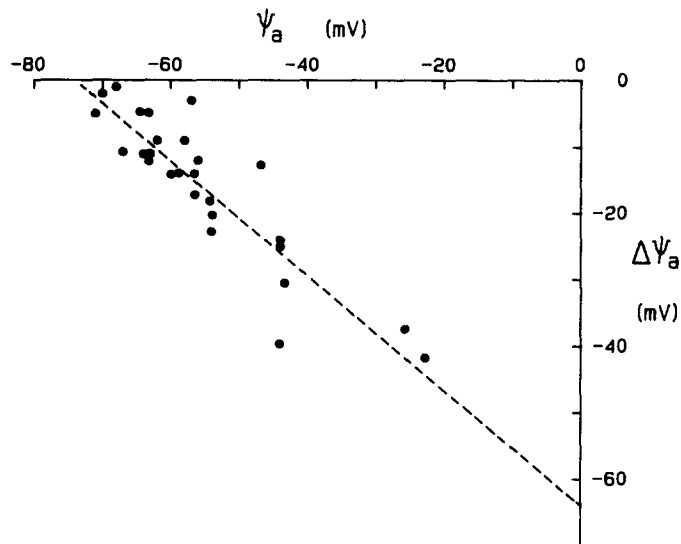


FIGURE 8. Relation of the hyperpolarization of ψ_a ($\Delta\psi_a$), induced by mucosal bumetanide (10^{-4} M), to the initial (control) ψ_a value. The line was drawn from a least-squares fit of data from 27 tissues.

30–40 mV during transport inhibition. A linear regression fit of the data yields a ψ_a intercept (i.e., that value of ψ_a at which no hyperpolarization would occur) of -74 mV. This value approximates the E_a^K (76 mV) of control tissues, determined by Smith et al. (26) using K-selective microelectrodes. In the presence of furosemide, E_a^K was 77 ± 3 mV ($n = 4$). Thus, ψ_a approaches E_a^K , which suggests that the apical membrane retains its high relative K conductance during inhibition of apical NaCl entry.

The effects of transport inhibitors in the presence of mucosal Ba are also consistent with this notion. Apical K conductance is reflected by the relation of ψ_a to $[K]_m$. Blockage of G_a^K by mucosal Ba results in a loss of K dependence of ψ_a at low $[K]_m$; under these conditions, the electrical potential profile is dominated by E_b^{Cl} (10). These findings were reproduced in a different series of experiments

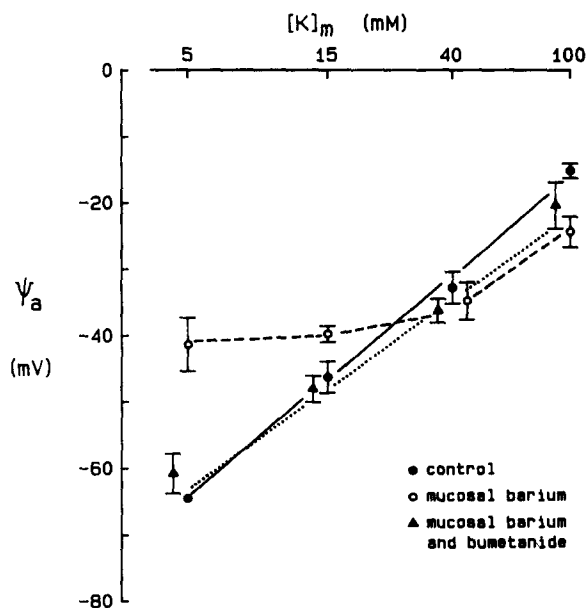


FIGURE 9. Relation of ψ_a to $[K]_m$ in control tissues, in the presence of mucosal Ba (2 mM) or Ba plus mucosal bumetanide (10^{-4} M). The means \pm SEM of values from three tissues are provided. Slopes of the relations, determined by least-squares fit, were: 37 mV/decade, control; 7 mV/decade, mucosal Ba; 31 mV/decade, mucosal Ba and bumetanide.

and the data are illustrated in Fig. 9. When bumetanide was added to the mucosal solution in the presence of Ba, the K dependence of ψ_a returned. In the presence of bumetanide, changes in $[K]_s$ did not alter ψ_b , so that, as in control tissues, a basolateral K conductance could not be detected.

The effects of bumetanide on cell Cl activity (a_c^{Cl}) are summarized in Table III. Changes in the electrical potential profile were similar to those presented earlier (Figs. 1 and 2). Under control conditions, cell Cl activity was slightly lower, and E_b^{Cl} correspondingly higher, than the values of 24 ± 3 mM and 41 ± 3 mV reported by Duffey et al. (3) (see also Table III of the preceding paper). Bumetanide decreased a_c^{Cl} to 11 ± 2 mM, a value not significantly different from

TABLE III
Effect of Bumetanide on the Electrical Potential Profile and Cell Cl Activities in Flounder Intestine

	ψ_t	ψ_a	a_c^{Cl}	E_b^{Cl}	ψ_b
	mV	mV	mM	mV	mV
Control	-4.0 ± 0.8	-63 ± 2	19 ± 2	48 ± 3	-59 ± 1
Bumetanide	$-0.8 \pm 0.1^*$	$-70 \pm 1^*$	$11 \pm 2^*$	$62 \pm 4^*$	$-69 \pm 1^*$

Means \pm SEM of five experiments. Bumetanide (0.1 mM) was added to mucosal solution alone. E_b^{Cl} was calculated as described previously (Table III; reference 10).

* $P < 0.05$ compared to control value.

that expected for a passive distribution of Cl across the limiting membranes (8 ± 2 mM). Accordingly, E_b^{Cl} approached ψ_b as a_c^{Cl} fell.

Fig. 10 provides measurements of fractional apical membrane resistance (f_a^R)

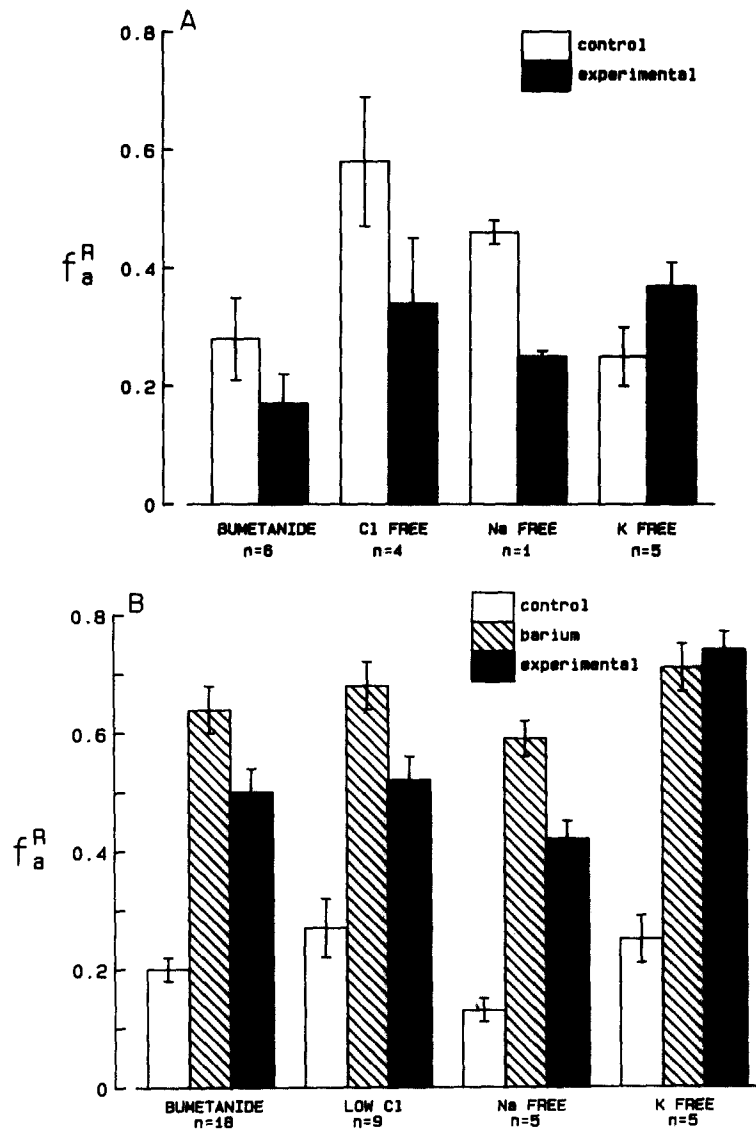


FIGURE 10. Effects of mucosal bumetanide (10^{-4} M) and ion replacement on f_a^R . (A) Control; (B) 2 mM Ba present in the mucosal solution during the "barium" and "experimental" periods. See the legend of Fig. 1 for solution composition. Means \pm SEM are provided, except for the control Na-free studies, where the range of values is given. Several tissues of the control group (A) employed for the Cl-free studies exhibited higher-than-normal f_a^R values. The effects of bumetanide and Cl-free solution are significant on a paired basis; variance is primarily between tissues (10).

with ion replacement and bumetanide in a format similar to the results shown earlier for ψ_a (Figs. 1 and 2). As illustrated in Fig. 10A, when apical salt entry is inhibited by bumetanide or either Cl or Na replacement, f_a^R decreases. Similar results were obtained when co-transport was inhibited by cGMP (Table II). The increase in f_a^R observed with K-free mucosal solutions is the response expected for removal of a permeant ion and does not conform to the pattern established for inhibition of apical salt entry. The results of Fig. 10B show that this pattern is retained in the presence of mucosal Ba: f_a^R decreases on exposure to mucosal bumetanide or Cl or Na replacement. However, the elevation of f_a^R induced by mucosal Ba is not reversed when the mucosal solution is rendered K-free, which again suggests an effective apical K channel blockade.

The decrease in f_a^R during transport inhibition implies a primary increase in

TABLE IV
Effects of Bumetanide and cGMP on Cellular Conductances in Flounder Intestine

	$\Delta\psi_t$		$\Delta\psi_a$	f_a^R	G_p/G_t	G_c	G_a	G_b
	Without Ba	With Ba						
	mV	mV	mV			mS/cm ²	mS/cm ²	mS/cm ²
Control (10)	4.6±0.2	2.2±0.2	38±1	0.39±0.04	0.95±0.00	1.9±0.2	4.8±0.3	2.7±0.4
Bumetanide (10)	2.4±0.1*	2.0±0.1	46±2*	0.24±0.02*	1.00±0.00*	0.3±0.1*	1.0±0.1*	0.3±0.1*
Control (10)	4.9±0.2	2.4±0.2	37±1	0.38±0.03	0.95±0.00	1.4±0.1	3.4±0.3	2.3±0.2
cGMP (7)	2.5±0.1*	2.1±0.1	48±1*	0.19±0.02*	0.99±0.00*	0.2±0.1*	1.5±0.1*	0.3±0.1*

Means ± SEM for the number of experiments given in parentheses. $\Delta\psi$ is the change in transepithelial or apical membrane potential elicited by raising $[K]_m$ from 5 to 40 mM. Bumetanide (0.1 mM) was added to the mucosal solution; 8-bromo-cGMP (0.05 mM) was added to the serosal solution; Ba (2 mM) was added to the mucosal solution.

* $P < 0.05$ compared to control.

apical conductance, G_a , or a decrease in basolateral conductance, G_b . An independent estimate of cellular conductance, G_c , would permit localization of the primary conductance change since increased G_a or decreased G_b would have opposing effects on G_c . We used the response of ψ_t to elevated $[K]_m$ in the presence and absence of mucosal Ba (10) to estimate the distribution of tissue conductance between cellular (G_c/G_t) and paracellular (G_p/G_t) pathways during transport inhibition. The effects of bumetanide and cGMP on the conductance properties of flounder intestine, assessed using this approach, are provided in Table IV.

The response of ψ_t to elevated $[K]_m$ is reduced by ~50% when transport is inhibited by bumetanide or cGMP. This is due to a reduction in the extent to which changes in cellular emf (ΔE_a^K) influence ψ_t and is reflected by the changes in ψ_a and ψ_t elicited by elevated $[K]_m$. During transport inhibition, the ψ_a induced

by increasing $[K]_m$ was larger than the corresponding control value (e.g., 37 vs. 48 mV with cGMP), but the impact of this $\Delta\psi_a$ on $\Delta\psi_t$ was reduced (4.9 vs. 2.5 mV). This could result from a decrease in G_c or an increase in G_p ; either would increase G_p/G_t as observed. However, a primary increase in G_p is unlikely since the control G_p/G_t was 0.95 and neither bumetanide nor cGMP significantly affects G_t (7, 21).

From the measured G_t values, we calculate that cellular conductance decreased by ~85% in response to bumetanide or cGMP. Since f_a^R also decreases, the primary change in the cellular pathway is a nearly 10-fold decrease in basolateral membrane conductance. However, the reduction in G_c that emerges from this analysis is so large that a significant decrease in apical membrane conductance is also implied.

DISCUSSION

In this section, we discuss: (a) the mechanistic features of the hyperpolarization of ψ_a and ψ_b that accompany inhibition of NaCl absorption across the apical membranes of flounder intestinal cells, (b) the role of conductance changes in modifying the cellular electrical potential profile, (c) the data that implicate a K-independent NaCl entry process, and (d) the possible physiological significance of a link between the electrical potential profile and apical salt entry.

Mechanism of the Hyperpolarization ($\Delta\psi_a$)

A number of observations indicate that hyperpolarization of ψ_a accompanies inhibition of coupled NaCl entry across the apical membrane. First, replacement of those mucosal solution ions that are involved in co-transport entry induce the $\Delta\psi_a$ (Fig. 1) and do so in a concentration-dependent fashion (Fig. 7). Second, bumetanide, an inhibitor of NaCl co-transport, mimics the effects of ion replacement. As the mucosal bumetanide concentration is increased, ψ_a hyperpolarizes and ψ_t decreases in parallel (Fig. 2). Finally, apical NaCl entry also is inhibited by cGMP, which induces a hyperpolarization of ψ_a that is similar in magnitude and time course to that observed with ion replacement or bumetanide (Table II). Each of these findings illustrates a direct relation between co-transport activity and ψ_a . They suggest that the electrical consequences of mucosal solution Na or Cl replacement are due to a decrease in coupled NaCl influx rather than to the presence of significant apical conductances to these ions.

The factors that determine ψ_a are expressed by Eq. 1, which incorporates our findings (10) of apical K and basolateral Cl conductances, to facilitate discussion of the $\Delta\psi_a$ that accompanies transport inhibition:

$$\psi_a = -(1 - f_a^R)E_a^K - f_a^R(E_b^{Cl} - \psi_t). \quad (1)$$

Since the limiting membranes remain selective for K and Cl, the electrical potential profile will be influenced by the same factors that determine the control ψ_a and ψ_b values. Cell K activity and E^K remain high (see Results, p. 10), probably because mechanisms that would lead to Na entry (to replace cell K) are blocked. Conversely, cell Cl activity decreases toward electrochemical equilibrium when apical NaCl co-transport is inhibited by Na replacement (3) or bumetanide (Table

III). This probably results from a transient imbalance in which NaCl and/or KCl exit continues after entry has ceased, and may be associated with a decrease in cell volume (27). As a_c^{Cl} falls, E^{Cl} rises so that at equilibrium, in the absence of transepithelial ion gradients, $E^{Cl} \cong E^K \cong \psi_a \cong \psi_b$ (as with bumetanide or cGMP). Thus, the approach of E^{Cl} toward E^K (Eq. 1) results in steady state hyperpolarization of the cellular electrical potential profile during transport inhibition. The time course of hyperpolarization will be influenced by conductive and co-transport pathways (e.g., G_b^{Cl} and basolateral KCl co-transport) that can facilitate the approach of a_c^{Cl} toward equilibrium levels.

Conductance Changes During Transport Inhibition

In addition to the increase in E^{Cl} , co-transport inhibition is associated with changes in cellular conductance, but bumetanide and cGMP inhibit an entry process which, on kinetic grounds, appears to be electrically neutral (17). The results of the analysis based on experimentally induced changes in E^K (Table IV) suggest that the decrease in f_a^R observed with co-transport inhibition is associated with a primary decrease in basolateral membrane conductance. Since the basolateral membrane is normally conductive to Cl, this implies that reduced apical NaCl entry inhibits G_b^{Cl} .

Two factors should be considered in reaching this conclusion. First, Ba may not completely block G_a^K and eliminate G_c , as assumed in the analysis of G_p/G_t (10) since bumetanide increases the K dependence of ψ_a , even in the presence of mucosal Ba (Fig. 9). However, increased K dependence of ψ_a will result from a decrease in f_a^R that is due to a primary decrease in G_b as well as from an increase in G_a^K per se. A decreased G_b would augment the relative apical membrane conductance so that the influence of any G_a^K that persists in the presence of mucosal Ba is enhanced. The conclusion that the decrease in f_a^R during transport inhibition is not due to an increase in G_a^K is supported by the decrease in K selectivity of the epithelium; that is, the $\Delta\psi_t$ induced by elevated $[K]_m$ decreases. In the presence of Ba, the $\Delta\psi_t$ values of control and inhibitor-treated tissues would be expected to differ if bumetanide and cGMP increased G_a^K , but they did not (Table IV). In addition, a significant residual G_c in the presence of Ba would lead to an underestimation of G_p/G_t (a change in ψ_t resulting from residual cellular conductance would be attributed to the paracellular pathway). Since the G_p/G_t values calculated for bumetanide and cGMP are close to unity (Table IV), the error introduced by any remaining G_c is small.

Second, the observed decrease in a_c^{Cl} , together with a Cl-conductive basolateral membrane, would account for part of this decrease in G_b . Using the Goldman equation, we calculate that G_b would fall by 25–50% as a_c^{Cl} drops during transport inhibition. The a_c^{Cl} values used in these calculations include the full range of control and equilibrium Cl activities found in this and earlier studies (3, 10). Thus, the effects of reduced permeant ion activity cannot account entirely for the nearly 10-fold reduction in G_b that emerges from the analysis of Table IV.

A decrease in G_b^{Cl} would be expected to prolong the decline in a_c^{Cl} toward equilibrium during inhibition of NaCl entry. Indeed, Duffey et al. (3) found that the half-time of decrease in a_c^{Cl} during mucosal solution Na replacement was

nearly 10 times that associated with the return of a_{c}^{Cl} to control levels upon re-exposure to Na-containing media. Factors that might regulate G_b^{Cl} and thereby serve as intracellular signals of reduced NaCl entry (or altered cell composition) are unknown at present.

The intracellular mediator(s) that regulates G_a^k is also unknown. Attempts to modify G_a^k by changing cell Ca or Ca-mediated regulatory processes have yielded uniformly negative results (11). The apparent decrease in G_a^k that accompanies cGMP- or bumetanide-induced inhibition of apical NaCl entry may reflect cyclic nucleotide regulation of apical K conductance, since guanylate cyclase activity has been identified in flounder intestinal cells (21). A decrease in G_a^k (26) and a twofold increase in cellular cGMP (21) accompany Na/K pump inhibition by ouabain. The decrease in cellular conductance that accompanies inhibition of salt absorption across flounder intestine may represent another instance of feedback regulation, which tends to preserve cell composition in the face of altered transepithelial transport. Feedback regulation of apical Na and basolateral K conductances in response to acute alterations in apical Na entry or Na/K pump activity is well documented (23, 25).

Involvement of K in the Response to Co-Transport Inhibition

To evaluate the role of K in the process whose inhibition leads to $\Delta\psi_a$, it was necessary to block G_a^k by adding Ba to the mucosal solution. In the presence of Ba, mucosal solution Na or Cl replacement or addition of bumetanide hyperpolarized ψ_a , but K replacement did not (Figs. 3 and 7). This suggests an effective blockade of apical K channels by Ba under these conditions, but also implies that the apical entry process, whose inhibition leads to $\Delta\psi_a$, is K-independent. Other evidence of a K-independent entry process also exists. Approximately 30–40% of transepithelial Cl transport and furosemide-sensitive Cl influx across the apical membrane persists after removal of K from the mucosal solution (16). In addition, a large fraction of ψ_t remains after mucosal solution K is replaced by Na (Fig. 4). The failure of K replacement to elicit $\Delta\psi_a$ through inhibition of Na/K/Cl co-transport cannot be attributed to a difference in the affinities of this process for K vs. Na, since the half-saturation concentrations (K_m) determined from unidirectional influx measurements (17) are similar ($K_m^K = 4$ mM and $K_m^{Na} = 3$ mM). The results of earlier studies suggest that when a solution with nominally zero [K] bathes the mucosal surface, the effective $[K]_m$ is ~ 1 mM (10). In the presence of mucosal Ba, an even lower $[K]_m$ can be expected since K leakage from the cells would be blocked. Thus, one can expect the activity of Na/K/Cl co-transport to be markedly reduced in the K substitution experiments of Fig. 3. This suggests that inhibition of Na/K/Cl co-transport alone is insufficient to hyperpolarize the apical membrane potential.

These findings raise the possibility that a K-independent NaCl entry process is capable of mediating apical salt uptake, particularly when K-dependent entry is compromised. It is difficult to know whether this is an ongoing process or is activated only when the Na/K/Cl entry rate falls, perhaps as a compensatory mechanism in cell volume regulation. Both NaCl entry processes appear to be sensitive to loop diuretics and cGMP since they decrease Cl uptake (7, 16) and elicit hyperpolarization of ψ_a . Thus, the only method of selectively suppressing

Na/K/Cl entry is K removal, which may simultaneously activate K-independent uptake. Cremaschi et al. (1) have reported different NaCl uptake mechanisms operating in parallel at the apical border of rabbit gallbladder. In addition, Spring and Ericson (27) have identified two different modes of NaCl entry at the apical membranes of *Necturus* gallbladder cells. A bumetanide-sensitive NaCl co-transport process functions in NaCl absorption under normal conditions. However, the volume-regulatory increase that accompanies exposure of this tissue to hypertonic media activates parallel Na/H and Cl/HCO₃ exchange processes, as judged by their sensitivity to amiloride and stilbenes. By analogy, flounder intestinal cells may have the capacity to activate another mode of NaCl entry when uptake via Na/K/Cl co-transport is compromised. Since luminal [K] varies between 1 and 5 mM in vivo (12, 19), the ability to activate a K-independent NaCl uptake process may be physiologically important for salt absorption from luminal solutions of low [K].

Physiological Significance of the Relation Between Co-Transport and ψ_a

A potential role of the coupling between NaCl entry and ψ_a concerns the mechanisms responsible for Na-coupled amino acid uptake from the intestinal lumen. Our results indicate that ψ_a lies between -75 and -110 mV when the mucosal surface is exposed to a solution that mimics luminal composition in vivo with [K]_m in the physiological range of 1-5 mM. This hyperpolarization of ψ_a (relative to the values observed when both surfaces are bathed by plasma-like solutions) would enhance the electrical gradient for Na-coupled absorption of neutral and positively charged amino acids. This may be particularly important in maintaining the driving force for amino acid uptake as luminal [Na] falls during absorption.

This work was supported by National Institutes of Health research grants AM 27524 and AM 31091 from the National Institute of Arthritis, Diabetes, and Digestive and Kidney Disease. Partial support of Drs. Halm and Krasny was provided by National Research Service Awards AM 06850 and AM 07306.

Original version received 2 August 1984 and accepted version received 28 January 1985.

REFERENCES

1. Cremaschi, D., G. Meyer, S. Bermano, and M. Marcati. 1983. Different sodium chloride cotransport systems in the apical membrane of rabbit gallbladder epithelial cells. *J. Membr. Biol.* 73:227-235.
2. Duffey, M. E., B. Hainau, S. Ho, and C. S. Bentzel. 1981. Regulation of epithelial tight junction permeability by cyclic AMP. *Nature (Lond.)*. 294:451-453.
3. Duffey, M. E., S. M. Thompson, R. A. Frizzell, and S. G. Schultz. 1979. Intracellular chloride activities and active chloride absorption in the intestinal epithelium of the winter flounder. *J. Membr. Biol.* 50:331-341.
4. Ellory, J. 1983. Inhibition of human red cell sodium potassium transport by divalent cations. *J. Physiol. (Lond.)*. 340:1-17.
5. Frizzell, R. A., M. Field, and S. G. Schultz. 1979. Sodium-coupled chloride transport by epithelial tissues. *Am. J. Physiol.* 236(Renal Fluid Electrolyte Physiol. 5):F1-F8.

6. Frizzell, R. A., D. R. Halm, M. W. Musch, C. P. Stewart, and M. Field. 1984. Potassium transport by flounder intestinal mucosa. *Am. J. Physiol.* 246(Renal Fluid Electrolyte Physiol. 15):F946–F951.
7. Frizzell, R. A., P. L. Smith, E. Vosburgh, and M. Field. 1979. Coupled sodium-chloride influx across brush border of flounder intestine. *J. Membr. Biol.* 46:27–39.
8. Garcia-Diaz, J. F., A. Corcia, and W. McD. Armstrong. 1983. Intracellular chloride activity and apical membrane chloride conductance in *Necturus* gallbladder. *J. Membr. Biol.* 73:145–155.
9. Greger, R., E. Schlatter, and F. Lang. 1983. Evidence for electroneutral Na:Cl cotransport in the cortical thick ascending limb of Henle's loop of rabbit kidney. *Pflügers Arch. Eur. J. Physiol.* 391:308–314.
10. Halm, D., E. J. Krasny, Jr., and R. A. Frizzell. 1985. Electrophysiology of flounder intestinal mucosa. I. Conductance properties of the cellular and paracellular pathways. *J. Gen. Physiol.* 85:843–864.
11. Halm, D. R., E. J. Krasny, Jr., and R. A. Frizzell. 1981. Apical membrane potassium conductance in flounder intestine: relation to chloride absorption. *Bull. Mt. Desert Isl. Biol. Lab.* 21:88–93.
12. Hickman, C. P., Jr. 1968. Ingestion, intestinal absorption, and elimination of seawater and salts in the southern flounder, *Paralichthys lethostigma*. *Can. J. Zool.* 46:457–466.
13. Katz, U., K. R. Lau, M. M. P. Ramos, and J. C. Ellory. 1982. Thiocyanate transport across fish intestine (*Pleuronectes platessa*). *J. Membr. Biol.* 66:9–14.
14. Kirsch, R., and M. F. Meister. 1982. Progressive processing of ingested water in the gut of sea-water teleosts. *J. Exp. Biol.* 98:67–81.
15. Krasny, E. J., Jr., J. Madara, D. R. DiBona, and R. A. Frizzell. 1983. Cyclic-AMP regulates tight junction permselectivity in flounder intestine. *Fed. Proc.* 42:1100. (Abstr.)
16. Musch, M. W., S. A. Orellana, L. S. Kimberg, M. Field, D. R. Halm, E. J. Krasny, Jr., and R. A. Frizzell. 1982. Na:K:Cl cotransport in the intestine of a marine teleost. *Nature (Lond.)* 300:351–353.
17. Musch, M. W., M. C. Rao, M. Field, D. R. Halm, and R. A. Frizzell. 1983. Potassium influx across flounder intestinal brush border: sodium and chloride dependence and effect of ouabain. *Fed. Proc.* 42:988. (Abstr.)
18. Oberleithner, H., G. Giebisch, F. Lang, and W. Wang. 1982. Cellular mechanism of the furosemide sensitive transport system in the kidney. *Klin. Wochenschr.* 60:1173–1179.
19. Parmelee, J. T., and J. L. Renfro. 1983. Esophageal desalination of seawater in flounder: role of active sodium transport. *Am. J. Physiol.* 245(Regulatory Integrative Comp. Physiol. 14):R888–R893.
20. Petersen, K., and L. Reuss. 1983. Cyclic-AMP induced chloride permeability in the apical membrane of *Necturus* gallbladder epithelium. *J. Gen. Physiol.* 81:705–729.
21. Rao, M. C., N. T. Nash, and M. Field. 1984. Differing effects of cGMP and cAMP on ion transport across flounder intestine. *Am. J. Physiol.* 246(Cell Physiol. 15): C167–C171.
22. Sackin, H., N. Morgunov, and E. Boulpaep. 1982. Electrical potentials and luminal membrane ion transport in the amphibian renal diluting segment. *Fed. Proc.* 41:1495. (Abstr.)
23. Schultz, S. G. 1981. Homocellular regulatory mechanisms in sodium-transporting epithelia: avoidance of extinction by "flush through." *Am. J. Physiology.* 241:F579–F590.
24. Sleet, R. B., and L. S. Weber. 1982. The rate and manner of seawater ingestion by a marine teleost and corresponding seawater modification by the gut. *Comp. Biochem. Physiol.* 72A:469–475.

25. Smith, P. L., and R. A. Frizzell. 1984. Chloride secretion by canine tracheal epithelium. IV. Basolateral membrane K permeability parallels secretion rate. *J. Membr. Biol.* 77:187-199.
26. Smith, P. L., M. W. Welsh, C. D. Stewart, R. A. Frizzell, S. A. Orellana, and M. Field. 1980. Chloride absorption by the intestine of the winter flounder *Pseudopleuronectes americanus*: mechanism of inhibition by reduced pH. *Bull. Mt. Desert Isl. Biol. Lab.* 20:96-101.
27. Spring, K. R., and A. Ericson. 1982. Epithelial cell volume modulation and regulation. *J. Membr. Biol.* 69:167-176.